Related Commentary on page 1775

American Journal of Pathology, Vol. 168, No. 6, June 2006

DOI: 10.2353/ajpath.2006.051316

Musculoskeletal Pathology

Age-Dependent Effect of Myostatin Blockade on Disease Severity in a Murine Model of Limb-Girdle Muscular Dystrophy

Stephanie A. Parsons,* Douglas P. Millay,*† Michelle A. Sargent,* Elizabeth M. McNally,‡ and Jeffery D. Molkentin*

From the Cincinnati Children's Hospital Medical Center, Cincinnati, Ohio; the Department of Molecular Genetics, Biochemistry, and Microbiology,† University of Cincinnati, Cincinnati, Ohio; and the Department of Medicine,‡ The University of Chicago, Chicago, Illinois*

Myostatin (MSTN) is a muscle-specific secreted peptide that functions to limit muscle growth through an autocrine regulatory feedback loop. Loss of MSTN activity in cattle, mice, and humans leads to a profound phenotype of muscle overgrowth, associated with more and larger fibers and enhanced regenerative capacity. Deletion of MSTN in the *mdx* mouse model of Duchenne muscular dystrophy enhances muscle mass and reduces disease severity. In contrast, loss of MSTN activity in the dy^{W}/dy^{W} mouse model of laminin-deficient congenital muscular dystrophy, a much more severe and lethal disease model, does not improve all aspects of muscle pathology. Here we examined disease severity associated with *myostatin* ($mstn^{-/-}$) deletion in mice nullizygous for δ-*sarcoglycan* ($scgd^{-/-}$), a model of limb-girdle muscular dystrophy. Early loss of MSTN activity achieved either by monoclonal antibody administration or by gene deletion each improved muscle mass, regeneration, and reduced fibrosis in $scgd^{-/-}$ mice. However, antibody-mediated inhibition of MSTN in late-stage dystrophic $scgd^{-/-}$ mice did not improve disease. These findings suggest that MSTN inhibition may benefit muscular dystrophy when instituted early or if disease is relatively mild but that MSTN inhibition in severely affected or late-stage disease may be ineffective. *(Am J Pathol 2006, 168:1975–1985; DOI: 10.2353/ajpath.2006.051316)*

Myostatin (MSTN), also known as growth and differentiation factor-8 (GDF-8), is a member of the transforming growth factor-β superfamily of growth factors and functions as a negative regulator of muscle mass.[1] Spontaneous mutations in the MSTN gene in mice and cattle have been demonstrated to lead to significantly greater muscle mass due to both muscle hypertrophy and hyperplasia.[2–5] Because of this role, inhibition of MSTN is a potentially important mechanism for treating human diseases that lead to muscle wasting and degeneration, such as muscular dystrophy.

The *mdx* (X-chromosome-linked muscular dystrophy) mouse is a well-characterized and widely used model for the study of Duchenne muscular dystrophy (DMD). Disease in the *mdx* model shows a continuum of severity in different muscles based partially on use, with the diaphragm being the most affected, although these mice do not ultimately die prematurely like human DMD patients. Studies in *mdx* mice have suggested that inhibition of MSTN partially rescues muscular dystrophy. For example, genetic deletion of *mstn* in the *mdx* background attenuated the severity of muscular dystrophy and histopathology, as well as enhanced regeneration.[6,7] In support of this conclusion, treatment of *mdx* mice with a dominant-negative MSTN propeptide fusion protein or a blocking monoclonal antibody each ameliorated/attenuated dystrophic pathology.[8,9] In contrast, a recent study by Li and colleagues[10] examined loss of MSTN in a much more severe dystrophic mouse model, the laminin α2-deficient dy^{W}/dy^{W} mice. These mice have severe skeletal muscle degeneration and die at 3 to 6 weeks of age. Interestingly, loss of MSTN in dy^{W}/dy^{W} mice does enhance muscle formation and regeneration, but it does not ultimately rescue disease or obviate muscle pathology.[10]

Here we investigated another mouse model of muscular dystrophy associated with loss of δ-sarcoglycan (*scgd*). This protein is a member of the sarcoglycan com-

Supported by the National Institutes of Health (grants to J.D.M. and E.M.M. and training grant no. 5T32 HL07382 to S.A.P.).

Accepted for publication March 13, 2006.

Supplemental material for this article can be found at *http://ajp.amjpathol.org.*

Address reprint requests to Jeffery D. Molkentin, Cincinnati Children's Hospital Medical Center, 3333 Burnet Ave., ML7020, Cincinnati, OH 45229-3039. E-mail: jeff.molkentin@cchmc.org.

plex within the greater dystrophin-glycoprotein complex (DGC) that is composed of several muscle-specific, transmembrane proteins important for maintaining membrane stability. The loss of *scgd* causes reductions or complete loss of the other members of the sarcoglycan complex and, in turn, leads to disassembly of the DGC.[11,12] *Scgd*$^{-/-}$ mice have cardiomyopathy and muscular dystrophy (corresponding to a human limb-girdle myopathy) that has many hallmarks of progressive and lethal muscular dystrophy, including cell death, muscle regeneration, inflammation, and fibrosis, in addition to reduced survival.[11,12] Here, we describe the outcome of two strategies to inhibit MSTN activity in *scgd*$^{-/-}$ mice. The first approach involves inhibition of MSTN by administration of blocking antibodies, whereas the second involves crossing *mstn*$^{-/-}$ mice with *scgd*$^{-/-}$ mice to yield double-null mice. We find that the timing of MSTN inhibition in *scgd*$^{-/-}$ mice is critical, such that early inhibition is beneficial whereas treatment of more advanced disease has no beneficial effect.

Materials and Methods

Animals

mstn$^{-/-}$ mice were generously supplied by Dr. Se Jin Lee (The Johns Hopkins University, Baltimore, MD), and *scgd*$^{-/-}$ mice were described previously.[11,13] Mice of both genotypes were in the C57BL6 background, and littermates or appropriately aged animals in the same background were used for controls. All animals had free access to food and water, and all experimentation was performed in the Cincinnati Children's Hospital Research Foundation animal care facility in accordance with the guidelines of the National Institutes of Health. Experimental protocols were reviewed and approved by the Institutional Animal Care and Use Committee. Both male and female mice of ages specified in the text were used for all analyses.

Cardiotoxin-Induced Muscle Injury

The gastrocnemius muscle of adult mice of specified ages was injected with 0.1 ml of 10 mmol/L cardiotoxin diluted in phosphate-buffered saline (Calbiochem, San Diego, CA). Muscles were harvested 10 days after injection, fixed overnight in 10% buffered formalin, and embedded in paraffin. Sections were cut at a thickness of 6 μm and stained with hematoxylin and eosin.

Antibody Administration

The mouse anti-MSTN monoclonal blocking antibody (clone JA16; Wyeth Research, Collegeville, PA) was generated against recombinant MSTN and inhibits the binding of MSTN to its receptor ActRIIB. Two age groups of *scgd*$^{-/-}$ mice (4 and 20 weeks old) were treated with weekly intraperitoneal injections of blocking antibodies or control antibodies (dose, 60 mg kg^{-1}) for 3 months as described previously.[9] Animals were weighed weekly.

Echocardiography

Mice were anesthetized with 2% isoflurane, and hearts were visualized using an Agilent (Palo Alto, CA) Sonos 5500 instrument and a 15-MHZ transducer (Palo Alto, CA). Cardiac ventricular dimensions were measured on M-mode three times for the number of animals indicated.

Western Analysis

Muscle protein extracts were prepared by homogenizing quadriceps muscle in cell lysis buffer containing 20 mmol/L Tris, pH 7.4, 137 mmol/L sodium chloride, 25 mmol/L β-glycerophosphate, 2 mmol/L sodium pyrophosphate, 2 mmol/L ethylenediaminetetraacetic acid, 1 mmol/L sodium orthovanadate, 1% Triton X-100, 10% glycerol, 1 mmol/L phenylmethyl sulfonyl fluoride, 5 μg/ml leupeptin, 5 μg/ml aprotinin, and 2 mmol/L benzamidine. Proteins (80 μg) were resolved on a sodium dodecyl sulfate-10% polyacrylamide gel, transferred to a polyvinylidene difluoride membrane, and immunodetected by using an enhanced chemifluorescence kit as specified by the manufacturer (Amersham Biosciences, Piscataway, NJ). The following antibodies were used: α-tubulin monoclonal antibody, 1:5000 dilution (Santa Cruz Biotechnology, Santa Cruz, CA); myogenin polyclonal antibody, 1:500 (M-19, Santa Cruz); α-actinin polyclonal antibody, 1:500 (Sigma); GAPDH polyclonal antibody, 1:2500 (Fitzgerald Industries International, Concord, MA); MEF2 polyclonal antibody (C-21, Santa Cruz); and MSTN/GDF8 polyclonal antibody, 1:500 dilution (Abcam, Cambridge, MA). Western blot reactivity was quantified on a Storm860 PhosphorImager (Molecular Dynamics, Piscataway, NJ) using Image Quant software.

Histology

Paraffin-embedded sections (6 μm thick) were cut at the mid-belly of the muscle. Care was taken so that all muscles were harvested in a uniform manner and so that identical regions of muscle were compared between animals.

Metamorph Analysis

Masson's trichrome-stained gastrocnemius and diaphragm sections were photographed using an Olympus BX51 microscope in conjunction with an Olympus U-TVI X digital camera (Melville, NY). Images were acquired using MagnaFire Image Capture software. For each muscle section, multiple photographs were taken so as to represent the entire section. Images were then analyzed with MetaMorph 6.1 software (Universal Imaging Corp., Downingtown, PA). Threshold was established using the hue-saturation-intensity color model. For all images, the inclusive threshold range of 144 to 206 for hue and 0 to 255 for both saturation and intensity were used to include only the blue fibrotic areas in the analysis as percent relative blue staining.

Semiquantitative Reverse Transcriptase-Polymerase Chain Reaction (RT-PCR)

RNA was isolated from diaphragm muscle from three to four separate wild-type (WT), *mstn*$^{-/-}$, *scgd*$^{-/-}$, and *mstn*$^{-/-}$ *scgd*$^{-/-}$ mice using TRIzol reagent (Invitrogen, Carlsbad, CA) according to the manufacturer's instructions. cDNA synthesis was performed using SuperScript III first-strand synthesis system for RT-PCR (Invitrogen) according to the manufacturer's protocol. PCR cycling conditions for Pax7 consisted of 96°C for 25 seconds, 57°C for 30 seconds, and 72°C for 1 minute, for L7, 96°C for 25 seconds, 58°C for 30 seconds, and 72°C for 45 seconds, and M-cadherin, 95°C for 25 seconds, 67°C for 30 seconds, and 72°C for 30 seconds. Product was collected at cycles 20, 23, 27, 31, and 35. Primer sets were as follows: Pax7 (5′-TCGATTAGCCGAGTGCTCA-GAATCA-3′ and 5′-AGCTGCTCGGCTGTGAACG-3′), and L7 (5′-GAAGCTCATCTATGAGAAGGC-3′ and 5′-AAGACGAAGGAGCTGCAGAAC-3′). M-cadherin primers have been described previously.[14]

Determination of Hydroxyproline Content

The method used is a modified version of that described by Woessner.[15] Briefly, a small piece of diaphragm (~5 to 8 mg) or gastrocnemius (~15 to 25 mg) was weighed and placed into a glass Pyrex tube containing 500 μl (diaphragm) or 750 μl (gastrocnemius) 6 N HCl. The tubes were capped loosely and placed at 100°C overnight to completely hydrolyze the tissue. The following day the tubes were uncapped and placed in a dessicator containing NaOH pellets in an oven at 50°C under vacuum until dry (24 hours to 1 week) and then resuspended in 5 mmol/L HC1 (1 ml). An aliquot of sample (20 μl) was combined with 180 μl of milliQ H_2O in 12 × 75-mm glass tubes. To this, 100 μl of chloramine T solution was added [0.14 g chloramine T (C-9887; Sigma, St. Louis, MO), 2 ml H_2O, 8 ml hydroxyproline assay buffer]. After addition of chloramine T solution, 1.25 ml of Erlich's reagent was added.[15] The samples were then vortexed for 15 seconds and then incubated at 55°C for 20 to 25 minutes. Once cooled to room temperature, sample absorbance was read at 558 nm. A standard curve was run alongside the samples using *trans*-4-hydroxy-L-proline (H-6002, Sigma) standards (ranging from 0 to 4 μg) to determine hydroxyproline concentration. Readings were normalized to original tissue weight.

Results

MSTN Antibody Treatment Enhances Muscle Mass in Younger, but Not Older, Mice

We selected two age groups of *scgd*$^{-/-}$ mice (4 weeks and 20 weeks of age) for analysis to examine the effect of anti-MSTN antibody inhibition early in disease, as well as later when the disease was characterized by fibrotic and fatty tissue replacement. Groups consisted of 4 weeks control antibody (six males), 4 weeks MSTN antibody (five males, one female), 20 weeks control antibody (four males, two females), 20 weeks MSTN antibody (four males). Mice were administered a course of either MSTN antibody or control antibody once a week for a 3-month time period, as described previously.[9] At the end of the study, animals were sacrificed and the heart and gastrocnemius, plantaris, tibialis anterior, and quadriceps muscles were dissected out and weighed. In the 4-week age group, all skeletal muscles measured demonstrated significant gains in mass after the MSTN antibody treatment relative to muscles from control antibody-treated mice, while two of the four muscle groups also showed

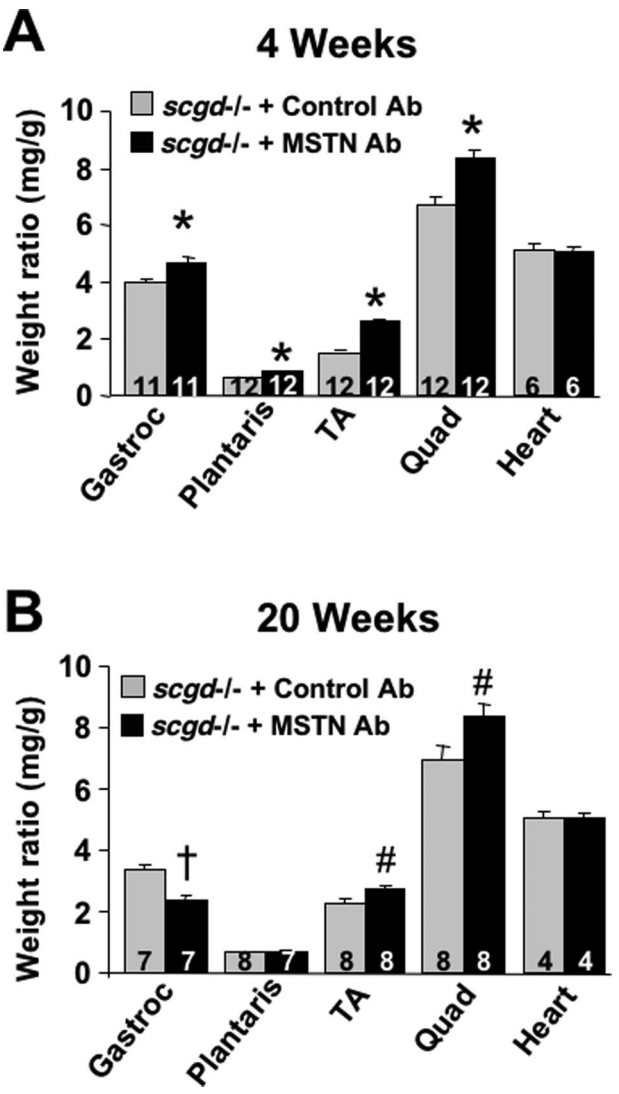

Figure 1. Comparison of relative muscle weights [muscle weight (mg)/body weight (g)] for gastrocnemius (gastroc), plantaris, tibialis anterior (TA), and quadriceps (quad) muscles and heart for *scgd*$^{-/-}$ mice treated with control or MSTN antibody beginning at either 4 weeks (**A**) or 20 weeks of age (**B**). Mice treated with MSTN antibody (Ab) beginning at 4 weeks showed gains in all skeletal muscles examined 12 weeks later (gastroc, $n = 11$; plantaris, $n = 12$; TA, $n = 12$; quad, $n = 12$; *t-test, $P < 0.01$), but no change was detected in the heart ($n = 6$). Mice treated with MSTN Ab beginning at 20 weeks showed gains in muscle weight for TA ($n = 8$) and quad ($n = 8$) only ($^{\#}P < 0.001$). Plantaris muscles showed no change ($n = 8$ control, $n = 7$ MSTN Ab), while gastrocnemius showed a significant loss of muscle weight ($n = 7$, $^{\dagger}P < 0.0006$). Again, no change in heart weight was detected ($n = 4$).

Table 1. Absolute Muscle and Body Weights in Control and MSTN Antibody-Treated Mice (Males Only)

	$scgd^{-/-}$ Control antibody	$scgd^{-/-}$ MSTN antibody
4 Weeks		
Gastrocnemius (mg)	119.68 ± 11.92 (n = 11)	155.07 ± 8.94 (n = 9)
Plantaris (mg)	20.64 ± 0.87 (n = 12)	28.95 ± 0.88 (n = 10)
TA (mg)	57.67 ± 2.47 (n = 12)	83.82 ± 3.27 (n = 10)
Quad (mg)	220.2 ± 9.69 (n = 12)	265.5 ± 12.51 (n = 10)
Heart (mg)	168.15 ± 8.14 (n = 6)	162.28 ± 5.63 (n = 5)
Body before (g)	17.87 ± 0.50 (n = 6)	15.38 ± 0.21 (n = 5)
Body after (g)	32.97 ± 0.91 (n = 6)	32.05 ± 0.50 (n = 5)
20 Weeks		
Gastrocnemius (mg)	124.57 ± 4.68 (n = 7)	80.09 ± 7.00 (n = 7)
Plantaris (mg)	25.03 ± 1.00 (n = 7)	24.13 ± 1.33 (n = 8)
TA (mg)	81.18 ± 6.58 (n = 8)	93.56 ± 6.18 (n = 8)
Quad (mg)	254.24 ± 12.25 (n = 8)	286.46 ± 19.37 (n = 8)
Heart (mg)	187.13 ± 10.71 (n = 4)	172.2 ± 8.03 (n = 4)
Body before (g)	35.15 ± 0.62 (n = 4)	33.15 ± 1.22 (n = 4)
Body after (g)	36.62 ± 0.72 (n = 4)	33.95 ± 1.77 (n = 4)

Raw muscle, heart, and body weights for the MSTN-treated mice beginning at 4 weeks or 20 weeks of age in $scgd^{-/-}$ receiving a nonspecific control antibody or MSTN antibody for 12 weeks. Muscle weights and heart weights were normalized to body weight and are presented in Figure 1 along with data from female mice, although this did not impact the data.

increased mass in the 20-week age group (Figure 1, A and B; Table 1). However, no significant differences were observed in relative heart weight between control antibody and MSTN antibody-treated mice (Figure 1, A and B; Table 1).

Administration of MSTN and Associated Muscle Pathological Changes

To observe changes in fibrosis associated with MSTN antibody treatment, sections from gastrocnemius and diaphragm were stained with Masson's trichrome. Despite increases in relative gastrocnemius weight in 4-week-old MSTN antibody-treated mice, there was no obvious alteration in the amount of collagen staining (Figure 2A). Amount of fibrosis assessed by MetaMorph software was comparable for both 4-week-old antibody-treated groups (Figure 2C). The validity of MetaMorph data were confirmed by comparing results to hydroxyproline assay results, both of which yielded nearly identical results (data not shown). Similar to the gastrocnemius, there was also no statistically significant difference in fibrosis in the diaphragms from 4-week-old MSTN antibody-treated mice, although there was a nonsignificant trend toward slightly more fibrosis (P = 0.1) (Figure 2, E and G). However, 20-week-old mice treated with MSTN antibody did show significant fibrotic tissue replacement ($P < 0.05$) (Figure 2B). Quantitation by MetaMorph revealed a 43% increase in fibrosis (Figure 2D). The same histopathology was observed for the diaphragm from older MSTN antibody-treated mice compared to control antibody treated $scgd^{-/-}$ mice, showing potentially more fibrosis (Figure 2, F and H). Again, histological data obtained from the gastrocnemius was validated by comparison with hydroxyproline assay results, which also suggested fulminant disease in the presence of MSTN inhibition (data not shown).

MSTN Antibody Treatment Increases Small-Diameter Fiber Populations in Both Age Groups Whereas Evidence for Increased Regeneration Is Found Only in Younger Mice

Analysis of muscle fibers from $scgd^{-/-}$ diaphragm revealed significant increases in populations of small-diameter fibers ($\leq$300 μm^2) relative to WT (Figure 3, A and B). Many of these fibers have centrally placed nuclei, an indirect indicator of muscle degeneration-regeneration. This increased number of regenerating fibers is thought to result from satellite cell proliferation and fusion to form early regenerating myotubes. Interestingly, in both young and old $scgd^{-/-}$ mice treated with MSTN antibody, there was an increase in the very smallest populations of fibers relative to control (Figure 3, A and B). These data would support the notion of increased activation and proliferation of satellite cells in response to MSTN inhibition. To further assess aspects of degeneration-regeneration, diaphragm sections were stained with wheat-germ agglutinin-tetramethyl-rhodamine isothiocyanate/bis-benzamide to visualize muscle fibers and nuclei to determine the percentage of total fibers containing centrally located nuclei. The 4-week group showed a significant increase in centrally nucleated fibers relative to their control antibody-treated counterparts (Figure 3C). However, the percentage of centrally located nuclei in diaphragm of control and MSTN antibody-treated mice in the 20-week-old treatment group was not different (Figure 3D) (see Discussion).

Deletion of mstn in $scgd^{-/-}$ Mice Enhances Muscle Mass and Cardiac Function

To better understand the consequences of MSTN inhibition in dystrophic skeletal muscle, we extended our studies *in vivo* by crossing $scgd^{-/-}$ mice with $mstn^{-/-}$

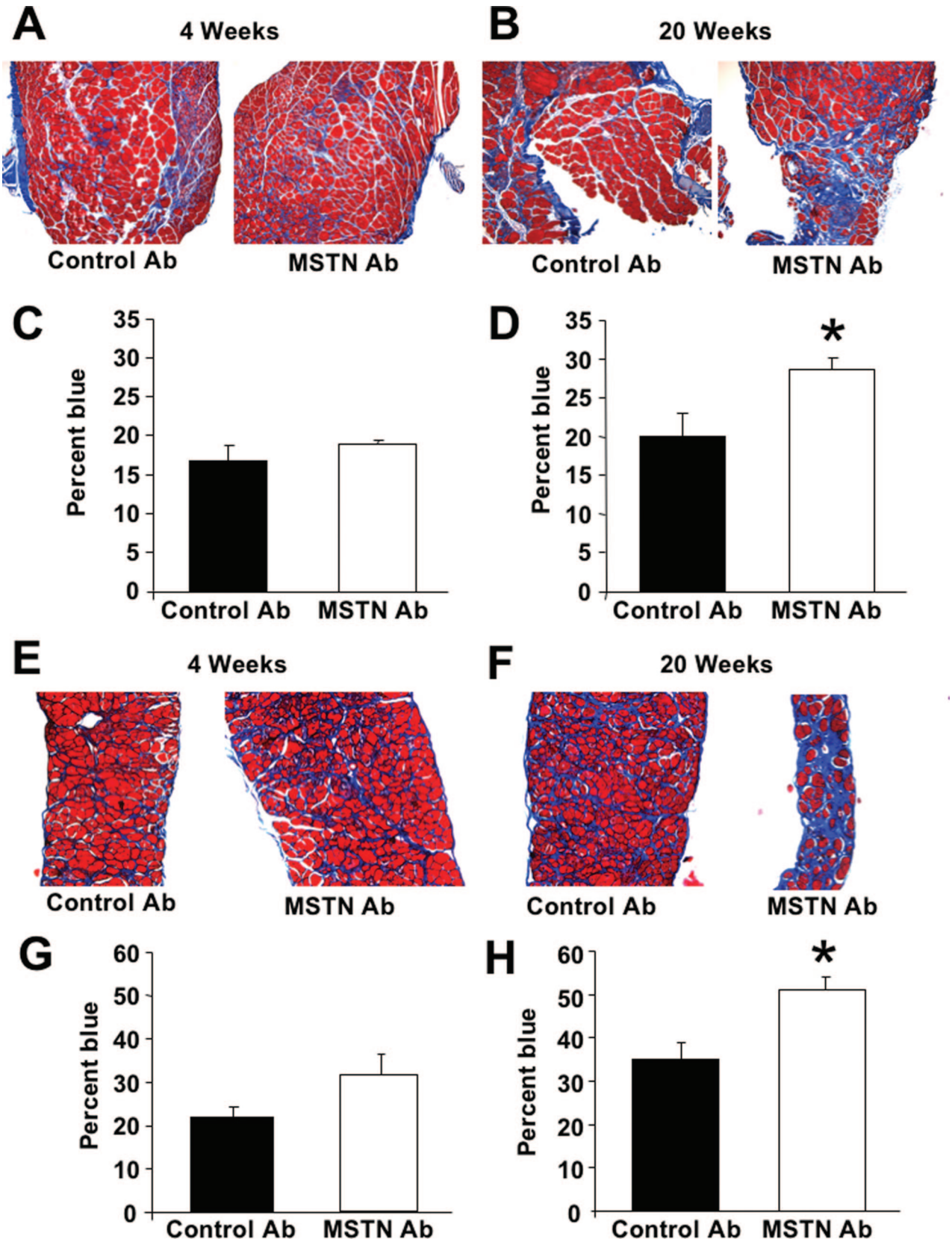

Figure 2. Analysis of Masson's trichrome-stained gastrocnemius and diaphragm sections for *scgd*$^{-/-}$ antibody-treated mice. Representative trichrome-stained sections of gastrocnemius muscle from control antibody (Ab) and MSTN Ab-treated mice beginning at 4 weeks (**A**) and 20 weeks (**B**) of age. MetaMorph 6.1 software quantification of area of fibrosis (blue staining) in gastrocnemius from animals Ab-treated beginning at 4 weeks (**C**) and 20 weeks (**D**) (*t-test, $P = 0.03$). Representative trichrome-stained sections of diaphragm muscle from control Ab and MSTN Ab-treated mice beginning at 4 weeks (**E**) and 20 weeks (**F**) of age. MetaMorph quantification of fibrosis in diaphragm from animals Ab-treated at 4 weeks (**G**) and 20 weeks (**H**) (*$P = 0.01$).

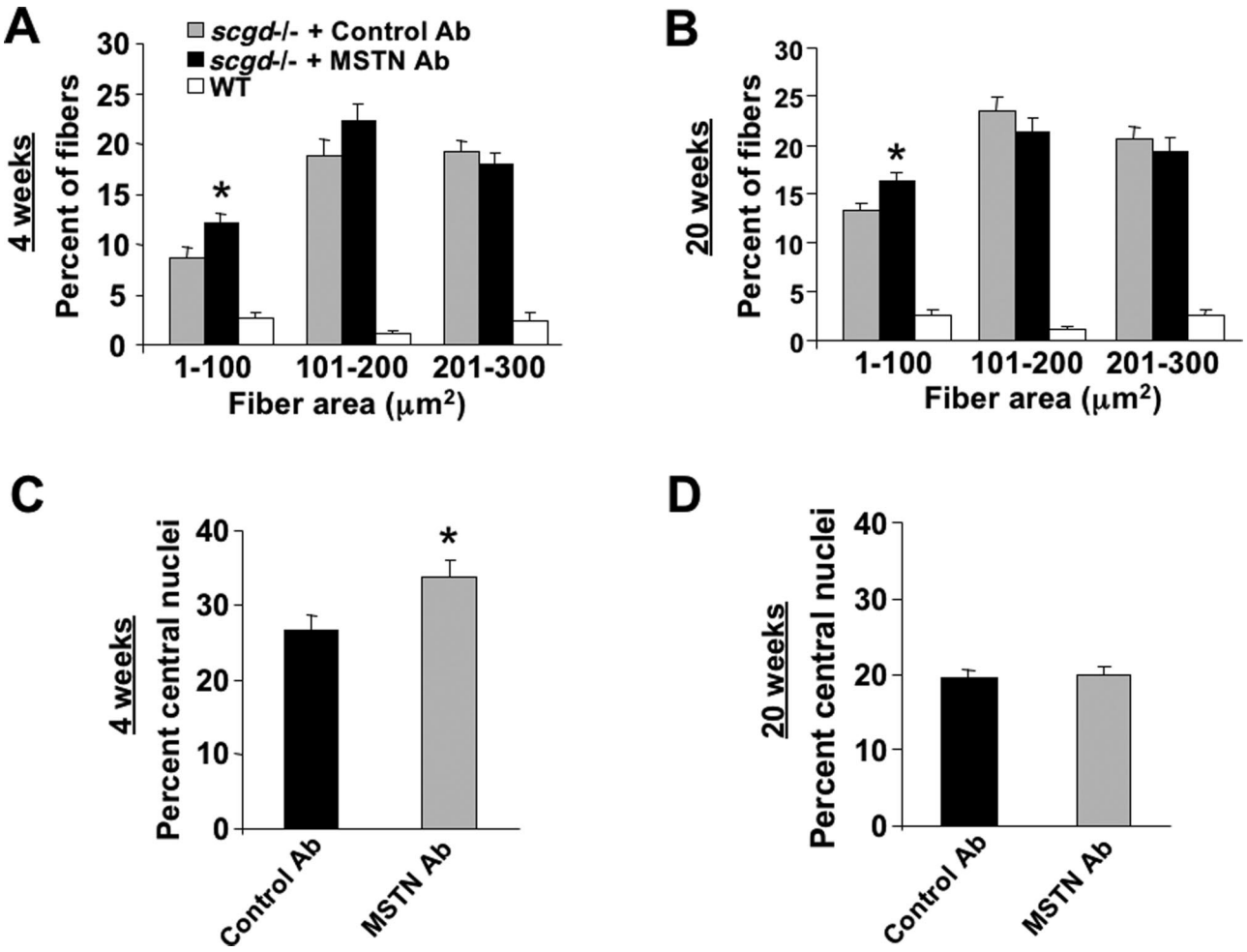

Figure 3. Muscle fiber areas and percent centrally nucleated fibers in $scgd^{-/-}$ mice treated with control antibody or MSTN antibody beginning at 4 weeks or 20 weeks of age. Diaphragm muscle fiber areas (μm^2) of mice treated beginning at 4 weeks (**A**) with control ($n = 6$) or MSTN antibody (Ab) ($n = 6$) (*t-test, $P = 0.01$) and at 20 weeks (**B**) with control ($n = 6$) or MSTN Ab ($n = 4$) (*$P = 0.03$). For all Ab-treated groups ~200 to 300 fibers were measured per field (×10 magnification), with two fields counted. Myofiber areas from WT ($n = 3$, >220 fibers/field, two fields) diaphragm, 31 weeks of age, were also measured to include as a nondiseased control. Percentage of fibers containing central nuclei in diaphragm muscle from mice treated with Ab beginning at 4 weeks (**C**) ($n = 5$, average 1100 fibers examined/mouse, *$P = 0.04$) or at 20 weeks (**D**) ($n = 4$, average 975 fibers examined/mouse).

mice to create $scgd^{-/-}$ $mstn^{-/-}$ double-targeted mice. We examined mice at ~36 weeks of age (±4 weeks), an age similar to the MSTN antibody-treated mice (20 weeks) when sacrificed (12 weeks later). We first examined levels of MSTN protein expression in WT, and dystrophic diaphragm muscle. MSTN protein levels were found to be dramatically decreased in dystrophic muscle, although there were no changes in other control proteins such as myocyte enhancer factor 2 (MEF2), myogenin, α-actinin, GAPDH, or α-tubulin (Figure 4A). As seen in previous studies, the gastrocnemius, quadriceps, and soleus muscles were all significantly larger in the absence of *mstn* compared with WT (Figure 4B, Table 2). However, the heart was not hypertrophic and was actually smaller when normalized to body weight, likely because $mstn^{-/-}$ mice have larger body weights (Figure 4B, Table 2). Absolute heart weight and heart weight relative to body weight or tibia length were not statistically different (Table 2 and data not shown).

We detected no significant difference between WT and $scgd^{-/-}$ quadriceps and soleus muscle weights, although gastrocnemius muscle weight was significantly decreased in $scgd^{-/-}$ mice (Figure 4B, Table 2). Conversely, $scgd^{-/-}$ mice showed cardiomyopathy and hypertrophic enlargement of the heart at later ages, as previously observed by us (E.M.M., unpublished results). The decrease in gastrocnemius muscle weight is reminiscent of the trend observed in 20-week-old MSTN antibody-treated $scgd^{-/-}$ mice (Figure 1B), possibly indicative of advanced muscle degeneration. Relative gastrocnemius and quadriceps muscle weights of $scgd^{-/-}$ $mstn^{-/-}$ mice, although not as great as $mstn^{-/-}$ mice, are significantly increased over $scgd^{-/-}$ muscles (Figure 4B, Table 2). Interestingly, average relative soleus weight is increased even above the average value of $mstn^{-/-}$ soleus weight (Figure 4B). Average relative heart weight was also higher than that seen in $mstn^{-/-}$ mice, suggesting that loss of MSTN did not prevent the development

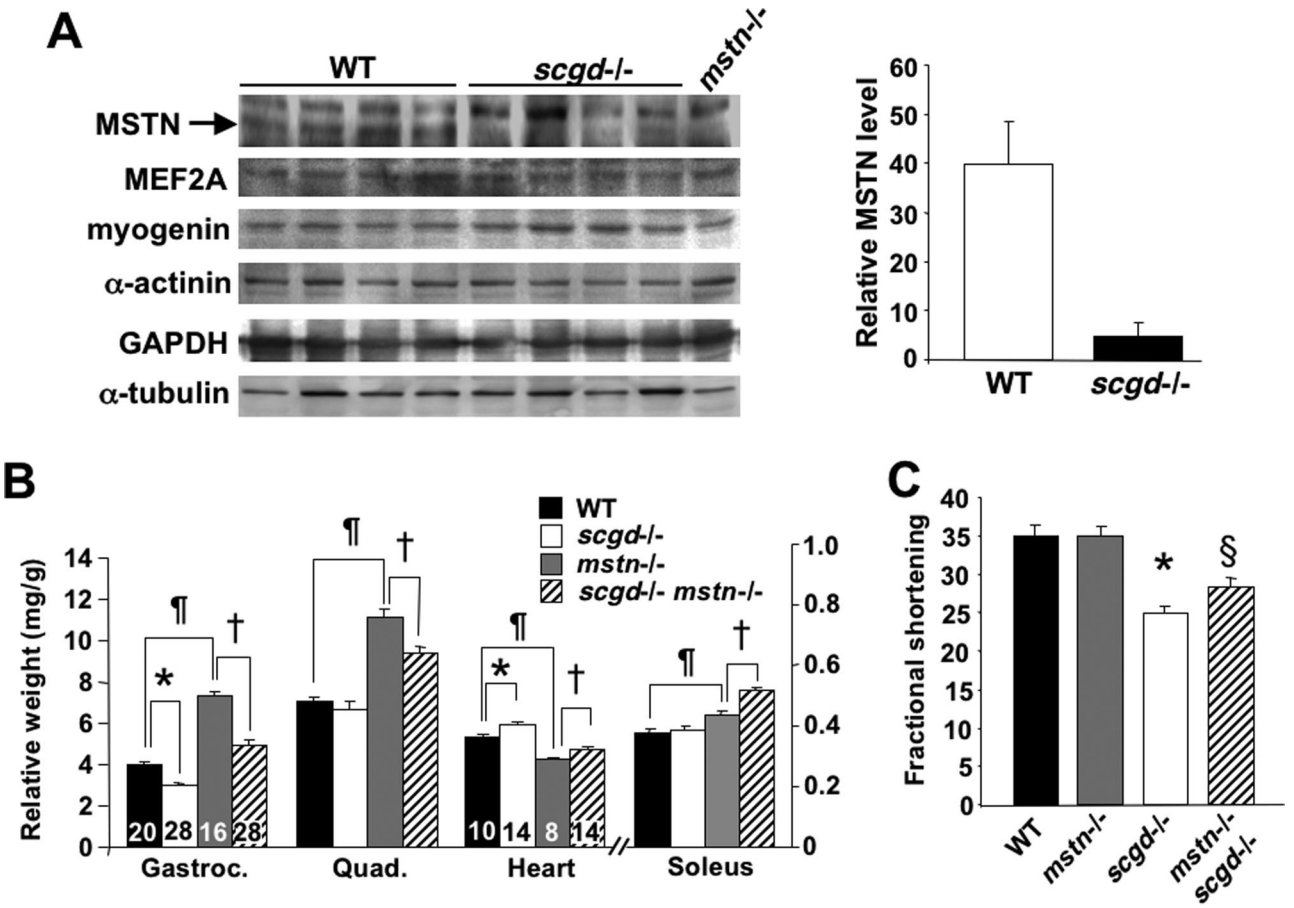

Figure 4. MSTN expression decreases in dystrophic muscle and loss of expression enhances relative muscle weight and improves cardiac function in *scgd*$^{-/-}$ *mstn*$^{-/-}$ mice. **A:** Western blot analysis of MSTN propeptide expression or the indicated control proteins in WT and *scgd*$^{-/-}$ quadriceps muscle (80 μg protein loaded). *mstn*$^{-/-}$ muscle was included as a negative control. Quantitation is shown in the graph on the **right**. **B:** Comparison of relative muscle weights for gastrocnemius, quadriceps, and soleus (WT, $n = 20$; *scgd*$^{-/-}$, $n = 28$; *mstn*$^{-/-}$, $n = 16$; *scgd*$^{-/-}$ *mstn*$^{-/-}$, $n = 28$) and heart (WT, $n = 10$; *scgd*$^{-/-}$, $n = 14$; *mstn*$^{-/-}$, $n = 8$; *scgd*$^{-/-}$ *mstn*$^{-/-}$, $n = 14$) (*t-test, $P < 0.000001$ *scgd*$^{-/-}$ relative to WT, $^{¶}P < 0.01$ *mstn*$^{-/-}$ relative to WT, $^{†}P < 0.01$ *scgd*$^{-/-}$ *mstn*$^{-/-}$ relative to *mstn*$^{-/-}$, except heart, $P = 0.04$). **C:** Comparison of cardiac fractional shortening by echocardiography (*$P = 0.00001$ relative to WT, $^{§}P = 0.02$ relative to *scgd*$^{-/-}$).

of cardiomyopathy that accompanies loss of *scgd* expression.

To further examine the functional impact of loss of MSTN activity in the heart, echocardiographic analysis was performed at ~30 weeks of age to assess changes in fractional shortening. Fractional shortening in WT and *mstn*$^{-/-}$ mice were nearly identical, whereas *scgd*$^{-/-}$ animals showed a significant reduction in function (Figure 4C). Interestingly, although *scgd*$^{-/-}$ *mstn*$^{-/-}$ mice also showed reduced ventricular performance, there was a significantly, albeit slight, improvement compared to *scgd*$^{-/-}$ mice (Figure 4C).

Genetic Loss of Myostatin Activity Leads to Decreased Fibrosis and Increased Regeneration in Dystrophic Muscle

Antibody-mediated MSTN inhibition was of no pathological detriment when administered early in disease, but it had either no effect or possibly worsened disease when administered late. Because *scgd*$^{-/-}$ *mstn*$^{-/-}$ mice lack MSTN expression at all stages of growth and development, these mice likely benefit from a developmental effect that might impart protection even in late adulthood.

Table 2. Absolute Muscle and Body Weights in the Indicated Cohorts of Mice (Males Only)

	WT	*scgd*$^{-/-}$	*mstn*$^{-/-}$	*scgd*$^{-/-}$ *mstn*$^{-/-}$
Gastrocnemius (mg)	141.01 ± 3.02 ($n = 12$)	89.76 ± 8.62 ($n = 12$)	297.14 ± 9.76 ($n = 8$)	157.17 ± 5.46 ($n = 12$)
Soleus (mg)	12.78 ± 1.16 ($n = 12$)	11.85 ± 1.04 ($n = 12$)	23.58 ± 5.14 ($n = 8$)	15.93 ± 1.93 ($n = 12$)
Quadriceps (mg)	241.14 ± 5.68 ($n = 12$)	191.53 ± 26.23 ($n = 12$)	441.76 ± 14.96 ($n = 8$)	291.93 ± 7.75 ($n = 12$)
Heart (mg)	151.95 ± 21.82 ($n = 6$)	194.85 ± 4.14 ($n = 6$)	183.7 ± 13.28 ($n = 4$)	170.18 ± 11.43 ($n = 6$)
Body (g)	34.54 ± 1.39 ($n = 6$)	31.51 ± 1.23 ($n = 6$)	41.33 ± 1.84 ($n = 4$)	34.00 ± 1.92 ($n = 6$)

Raw muscle, heart, and body weights for the indicated groups of mice sacrificed at 36 weeks of age. Muscle weights and heart weights were normalized to body weight and are presented in Figure 4 with the addition of female mice, which did not alter the overall conclusions (males and females showed similar affects).

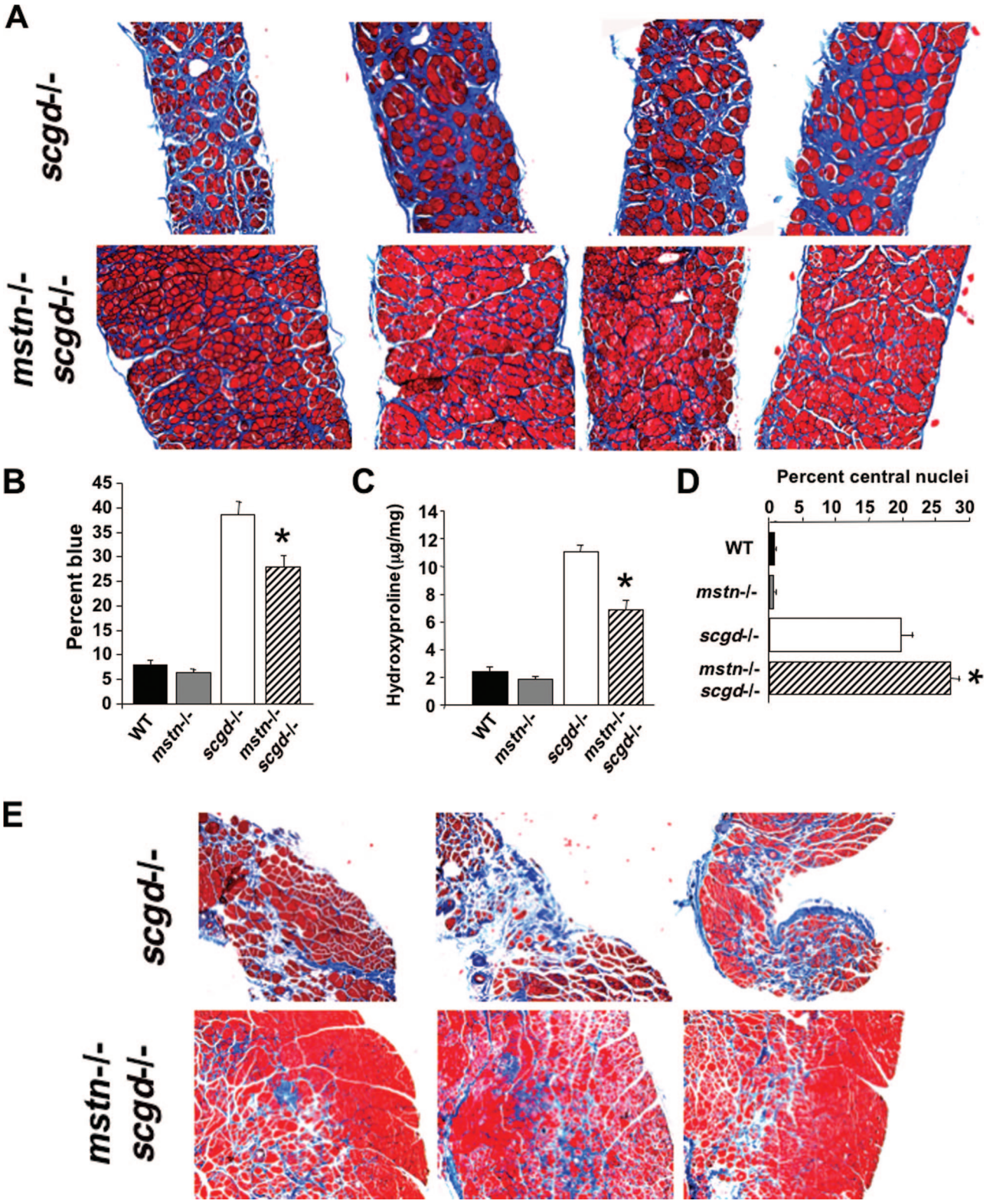

Figure 5. Analysis of Masson's trichrome-stained gastrocnemius and diaphragm sections for WT, *scgd*$^{-/-}$, *mstn*$^{-/-}$, and *scgd*$^{-/-}$ *mstn*$^{-/-}$ *mice*. **A:** Representative trichrome-stained sections of diaphragm muscle. **B:** MetaMorph quantification of area of fibrosis in diaphragm muscle (WT, $n = 3$; *mstn*$^{-/-}$, $n = 3$; *scgd*$^{-/-}$, $n = 12$; *scgd*$^{-/-}$ *mstn*$^{-/-}$, $n = 11$; *t-test, $P = 0.005$). **C:** Hydroxyproline assay data obtained from diaphragm muscle (WT, $n = 3$; *mstn*$^{-/-}$, $n = 3$; *scgd*$^{-/-}$, $n = 4$; *scgd*$^{-/-}$ *mstn*$^{-/-}$, $n = 5$; *$P = 0.002$ relative to *scgd*$^{-/-}$). **D:** Percentage of fibers containing central nuclei in diaphragm muscle (WT, $n = 4$; *mstn*$^{-/-}$, $n = 3$; *scgd*$^{-/-}$, $n = 3$; *scgd*$^{-/-}$ *mstn*$^{-/-}$, $n = 3$; average 640 fibers examined/mouse, *$P = 0.03$ relative to *scgd*$^{-/-}$). **E:** Representative trichrome-stained sections of gastrocnemius muscle.

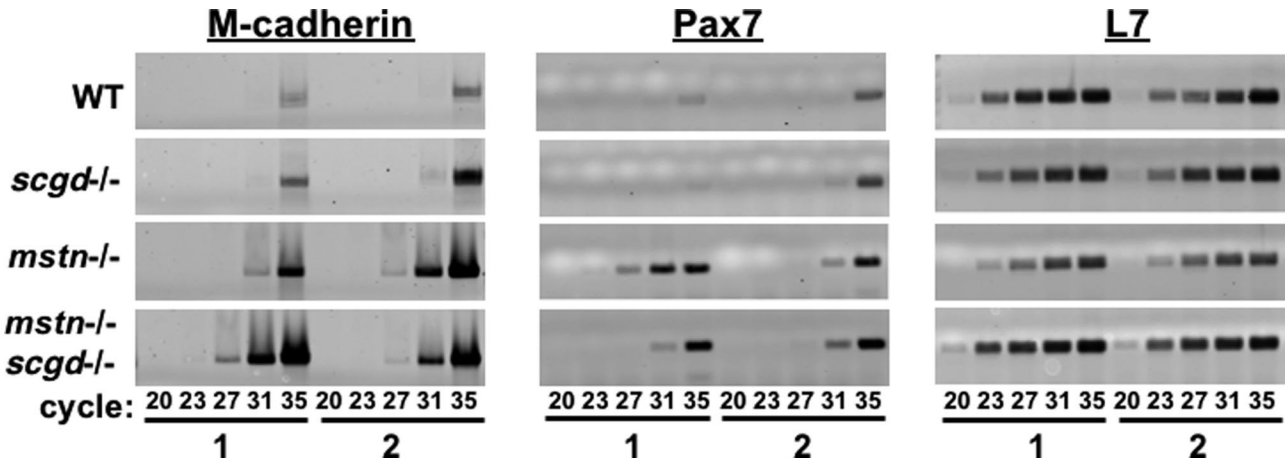

Figure 6. Representative semiquantitative RT-PCR data. Expression of satellite cell markers Pax7 and M-cadherin in diaphragm tissue of WT, *scgd*$^{-/-}$, *mstn*$^{-/-}$, and *scgd*$^{-/-}$ *mstn*$^{-/-}$ mice of ~36 weeks of age. Data are representative of that seen from analysis of three to four mice per genotype per marker, although data from only two mice in each group are shown (mouse 1 and mouse 2). L7 is a housekeeping control mRNA.

Indeed, Masson's trichrome staining of diaphragm sections revealed that muscle from *scgd*$^{-/-}$ *mstn*$^{-/-}$ mice contained more fibers than did those from *scgd*$^{-/-}$ mice (Figure 5A). Moreover, the double-null mice demonstrated noticeably less fibrosis, verified by MetaMorph quantitation (Figure 5B) as well as by hydroxyproline content (Figure 5C). Furthermore, analysis of diaphragm sections stained with wheat-germ agglutinin-tetramethylrhodamine isothiocyanate/bis-benzamide to visualize muscle fibers and associated nuclei showed that *scgd*$^{-/-}$ *mstn*$^{-/-}$ diaphragm contained more centrally-nucleated fibers, indicating increased regeneration (Figure 5D). There were also similar decreases in fibrosis in the gastrocnemius muscles of *scgd*$^{-/-}$ *mstn*$^{-/-}$ mice compared with *scgd*$^{-/-}$ mice alone (Figure 5E).

Expression of Satellite Cell Markers Is Increased in mstn-Deficient Tissue

The predominant mechanism by which loss of MSTN activity functions to benefit dystrophic muscle is still unclear. A previous study by McCroskery and colleagues[16] found that MSTN negatively regulates satellite cell self-renewal. Thus, loss of MSTN could further enhance satellite cell activity to benefit dystrophic muscle as previously proposed.[6] To examine this possibility we performed RT-PCR from WT, *scgd*$^{-/-}$, *mstn*$^{-/-}$, and *scgd*$^{-/-}$ *mstn*$^{-/-}$ diaphragm muscle to analyze two well-known satellite cell markers: M-cadherin and Pax7. Interestingly, in both dystrophic and WT muscle we found similar low levels of Pax7 and M-cadherin expression (Figure 6). However, *mstn*$^{-/-}$ and *scgd*$^{-/-}$ *mstn*$^{-/-}$ muscle showed increased expression of both satellite cell markers (Figure 6). These data suggest that *mstn* deletion may partially benefit disease in *scgd*$^{-/-}$ mice through enhanced satellite cell activity.

Discussion

Although the results reported in the *mdx* model are exciting and suggest that MSTN inhibition could benefit disease, some issues require discussion. First, *mdx* mice might have greater regenerative capacity in their skeletal muscle compared with humans with muscular dystrophy.[17–22] Second, *mdx* mice can show up-regulation of utrophin that may partially compensate for the lack of dystrophin, thus reducing pathological manifestations of disease somewhat. In contrast, humans with DMD show no significant utrophin up-regulation and are characterized by progressive muscle degeneration with satellite cell senescence.[20–22] Finally, progression of disease in human DMD patients leads to significantly shortened life expectancy, while *mdx* mice have a near-normal lifespan. On the other extreme, a recent study involving the genetic cross of a *laminin-α2*-deficient mouse and the *mstn*-null mouse observed no benefit to muscle necrosis and inflammation on MSTN inhibition, although indexes of regeneration and muscle size were increased.[10] However, the phenotype of *dy*^{w}/*dy*^{w} mice could have also been secondarily impacted by the loss of fat in the absence of *mstn*, thus possibly contributing to the observation of increased early neonatal lethality, in conjunction with defective skeletal muscle.[10] This last point notwithstanding, a case could be made that MSTN inhibition may not be beneficial in all dystrophic contexts.

Here we used the *scgd*$^{-/-}$ mouse model, which has a pathological course of disease that is intermediate between *mdx* and *dy*^{w}/*dy*^{w} mice. Loss of δ-sarcoglycan in the mouse models a form of human limb-girdle muscular dystrophy referred to as LGMD2F. However, loss of any of the proteins within the DGC, or other membrane-associated structural genes such as dystrophin, leads to a similar disease mechanism that involves destablization of the sarcolemma and influx of calcium, which induces apoptotic and necrotic cell death of myofibers. Thus, although the *scgd*$^{-/-}$ mouse model used here corresponds to a rare form of human disease, its use to dissect disease progression in the absence of MSTN is likely relevant to most forms of muscular dystrophy. Indeed, *scgd*$^{-/-}$ mice show both skeletal muscle and cardiac muscle disease, they show fairly widespread pathology in all skeletal muscles examined that is reminiscent of the

pathology observed in the most common human muscular dystrophies, and they have shortened lifespan as seen in many human muscular dystrophies such as DMD.[11,12]

In addition to disease severity as a potential variable for muscular dystrophy progression in association with MSTN inhibition, the timing of inhibition is also a critical variable that may indirectly reflect disease severity. For example, at 3 to 4 weeks of age *scgd*$^{-/-}$ mice undergo a typical severe bout of myofiber degeneration and subsequent regeneration, but after this initial period disease is more stable and is characterized by a gradual progression of pathology.[12] As *scgd*$^{-/-}$ mice age beyond 4 months muscle damage becomes more cumulative and is characterized by endomysial fibrosis, fiber splitting, dystrophic calcification, and fatty infiltration. The data presented here show that MSTN inhibition in young *scgd*$^{-/-}$ mice enhances muscle mass and indexes of regeneration. However, even at this early stage of treatment, MSTN inhibition had no effect on the fibrotic content of gastrocnemius and diaphragm, suggesting that there are early dystrophic changes that cannot be reversed by MSTN inhibition. By 20 weeks of age, most pathological changes appear relatively fulminant, such that MSTN inhibition was of no obvious benefit, despite leading to increased muscle mass in some muscles (tibialis anterior and quadriceps). Consistent with the study in the young *scgd*$^{-/-}$ mice, the more heavily used muscles such as the diaphragm and gastrocnemius showed even greater pathology and decreased relative muscle weight on MSTN inhibition from week 20 through week 32. It is important to note that we did not examine whether initiation of treatment with JA-16 at an earlier age could impact the pathology observed in the older mice. Ideally, treatment would have had to be initiated at 1 to 2 weeks of age, before significant disease is observed, and continued for 7 to 8 months.

The progression of disease in the mice analyzed here does not appear to be related to satellite cell exhaustion because the satellite cell markers Pax3, Pax7, and M-cadherin were not decreased in the diaphragm on MSTN inhibition (data not shown). This is further substantiated by the increased population of small-diameter fibers in MSTN-inhibited mice relative to control. Previous work has demonstrated that, in general, aged skeletal muscle does not regenerate as robustly as young skeletal muscle.[21] Indeed, we observed that our older group did not resolve a cardiotoxin injury response in the gastrocnemius as well as younger mice (Supplemental Figure 1 at *http://ajp.amjpathol.org*). Both WT and *scgd*$^{-/-}$ mice at 4 months of age showed good resolution of injury 10 days after cardiotoxin injection, while by 8.5 months the resolution was noticeably delayed and extensive histopathology was still present, especially in the *scgd*$^{-/-}$ mice (Supplemental Figure 1 at *http://ajp.amjpathol.org*). The reason for impaired regenerative ability with age is not completely understood, although recent studies suggest that there are modifications within the environment of aged muscle that affect activation of satellite cells.[22] For instance, the injury-specific induction of the Notch ligand Delta decreases with age, dramatically decreasing the regenerative capacity of the muscle.[23] Other circulating neuroendocrine factors likely underlie these affects because the systemic environment was shown to be critical for controlling the regenerative potential of satellite cells in old mice that shared a common circulation with young mice.[24] Consistent with these results, other endocrine/paracrine regulatory factors such as insulin-like growth factor-1 and hepatocyte growth factor are known to be important regulators of satellite cell activity and proliferation.[25–27]

Our working hypothesis is that the lack of rescue in the older *scgd*$^{-/-}$ mice after MSTN antibody treatment is related to myotube formation/differentiation in the context of aged dystrophic muscle. Differentiation is a process whereby myoblasts fuse to existing damaged fibers or to each other to form new primary myofibers. Whereas MSTN inhibition in young mice increased populations of myofibers containing central nuclei, mice treated with MSTN antibody at 20 weeks of age demonstrated no change in percentage of myofibers containing central nuclei. Thus, despite any positive effects on satellite cell proliferation, the incorporation of these cells into new fibers appears to be impaired, leading to an imbalance in the regenerative process. This impairment might be due to a progressive spatial separation and confinement of the satellite cells within the endomysial spaces of degenerated muscle fibers as well as by extreme interstitial fibrosis.[28] This defect in regenerative capacity might also be exacerbated by the advanced age of the muscle and accompanying decline of systemic factors (such as insulin-like growth factor-1 and hepatocyte growth factor). The net result of this impairment is continued degeneration and a progressive increase in fibrosis relative to control. Alternatively, there could be additional disease modifying secreted factors that change as dystrophy progresses to affect regenerative capacity. Indeed, human DMD patients surveyed throughout development show a progression in transforming growth factor-β levels in muscle that could also impact disease and satellite cell activity, although MSTN levels were not altered.[29]

In contrast to the phenotype observed in older *scgd*$^{-/-}$ mice treated with MSTN blocking antibody, deletion of the *mstn* gene in the *scgd*$^{-/-}$ background consistently improved pathology at all time points analyzed. On the surface, this later observation seems inconsistent with the antibody treatment study of older *scgd*$^{-/-}$ mice that showed either no effect or possibly worsening of disease. However, *mstn* gene disruption produces dramatic developmental effects that result in greater muscle fiber number[13] and greater satellite cell number.[16] Satellite cells from *mstn*$^{-/-}$ mice also showed increased proliferative ability that is associated with faster injury resolution.[16,30] Thus, genetic deletion of *mstn* may fundamentally alter the composition of muscle and satellite cells rendering muscle better able to deal with degenerative events or diseases throughout life. Another possibility is that increased muscle mass itself associated with *mstn* deletion leads to less overall stress per individual fiber because more overall fibers contribute to a contraction event, thus degeneration is slowed somewhat. However, despite these potentially favorable effects, *scgd*$^{-/-}$

mstn$^{-/-}$ mice still show significant disease because the underlying genetic defect is still present. Indeed, the gastrocnemius and quadriceps muscle from *scgd*$^{-/-}$ *mstn*$^{-/-}$ mice weighed significantly less than their *mstn*$^{-/-}$ counterparts. These observations can be explained because loss of MSTN does not correct the primary genetic defect, so although there is more muscle, it is nonetheless, defective.

In conclusion, our results in *scgd*$^{-/-}$ mice support the overall findings reported in *mdx* mice, suggesting that MSTN inhibition could be therapeutically beneficial for treating DMD if administered before disease progression becomes irreversible. Another important result is that MSTN inhibition with the blocking antibody (Figure 4C) or by gene deletion (data not shown) was of no detriment to the heart, and may even benefit it. However, skeletal muscle pathology was not favorably influenced by antibody-based MSTN inhibition in older *scgd*$^{-/-}$ mice in which disease was more firmly entrenched. To date, murine models suggest that MSTN inhibition, whether achieved pharmacologically or through selective gene deletion, will be more effective in less severe dystrophic diseases such as Becker-type muscular dystrophy, mild limb-girdle muscular dystrophies, or in young DMD patients that have not yet manifested more serious disease.

Acknowledgments

We thank Drs. Robert Mitchell and David L. Crandall at Wyeth Research, Collegeville, PA, for supplying the JA-16 monoclonal antibody and for helpful discussions.

References

1. Lee SJ: Regulation of muscle mass by myostatin. Annu Rev Cell Dev Biol 2004, 20:61–86
2. Grobet L, Martin LJ, Poncelet D, Pirottin D, Brouwers B, Riquet J, Schoeberlein A, Dunner S, Menissier F, Massabanda J, Fries R, Hanset R, Georges M: A deletion in the bovine myostatin gene causes the double-muscled phenotype in cattle. Nat Genet 1997, 17:71–74
3. Kambadur R, Sharma M, Smith TP, Bass JJ: Mutations in myostatin (GDF8) in double-muscled Belgian Blue and Piedmontese cattle. Genome Res 1997, 7:910–916
4. McPherron AC, Lee SJ: Double muscling in cattle due to mutations in the myostatin gene. Proc Natl Acad Sci USA 1997, 94:12457–12461
5. Szabo G, Dallmann G, Muller G, Patthy L, Soller M, Varga L: A deletion in the myostatin gene causes the compact (Cmpt) hypermuscular mutation in mice. Mamm Genome 1998, 9:671–672
6. Wagner KR, Liu X, Chang X, Allen RE: Muscle regeneration in the prolonged absence of myostatin. Proc Natl Acad Sci USA 2005, 102:2519–2524
7. Wagner KR, McPherron AC, Winik N, Lee SJ: Loss of myostatin attenuates severity of muscular dystrophy in mdx mice. Ann Neurol 2002, 52:832–836
8. Bogdanovich S, Perkins KJ, Krag TO, Whittemore LA, Khurana TS: Myostatin propeptide-mediated amelioration of dystrophic pathophysiology. FASEB J 2005, 19:543–549
9. Bogdanovich S, Krag TO, Barton ER, Morris LD, Whittemore LA, Ahima RS, Khurana TS: Functional improvement of dystrophic muscle by myostatin blockade. Nature 2002, 420:418–421
10. Li ZF, Shelton GD, Engvall E: Elimination of myostatin does not combat muscular dystrophy in dy mice but increases postnatal lethality. Am J Pathol 2005, 166:491–497
11. Hack AA, Lam MY, Cordier L, Shoturma DI, Ly CT, Hadhazy MA, Hadhazy MR, Sweeney HL, McNally EM: Differential requirement for individual sarcoglycans and dystrophin in the assembly and function of the dystrophin-glycoprotein complex. J Cell Sci 2000, 113:2535–2544
12. Coral-Vazquez R, Cohn RD, Moore SA, Hill JA, Weiss RM, Davisson RL, Straub V, Barresi R, Bansal D, Hrstka RF, Williamson R, Campbell KP: Disruption of the sarcoglycan-sarcospan complex in vascular smooth muscle: a novel mechanism for cardiomyopathy and muscular dystrophy. Cell 1999, 98:465–474
13. McPherron AC, Lawler AM, Lee SJ: Regulation of skeletal muscle mass in mice by a new TGF-β superfamily member. Nature 1997, 387:83–90
14. Beauchamp JR, Heslop L, Yu DS, Tajbakhsh S, Kelly RG, Wernig A, Buckingham ME, Partridge TA, Zammit PS: Expression of CD34 and Myf5 defines the majority of quiescent adult skeletal muscle satellite cells. J Cell Biol 2000, 151:1221–1234
15. Woessner Jr JF: The determination of hydroxyproline in tissue and protein samples containing small proportions of this imino acid. Arch Biochem Biophys 1961, 93:440–447
16. McCroskery S, Thomas M, Maxwell L, Sharma M, Kambadur R: Myostatin negatively regulates satellite cell activation and self-renewal. J Cell Biol 2003, 162:1135–1147
17. Tanabe Y, Esaki K, Nomura T: Skeletal muscle pathology in X chromosome-linked muscular dystrophy (mdx) mouse. Acta Neuropathol (Berl) 1986, 69:91–95
18. Anderson JE, Ovalle WK, Bressler BH: Electron microscopic and autoradiographic characterization of hindlimb muscle regeneration in the mdx mouse. Anat Rec 1987, 219:243–257
19. Cullen MJ, Jaros E: Ultrastructure of the skeletal muscle in the X chromosome-linked dystrophic (mdx) mouse. Comparison with Duchenne muscular dystrophy. Acta Neuropathol (Berl) 1988, 77:69–81
20. Decary S, Hamida CB, Mouly V, Barbet JP, Hentati F, Butler-Browne GS: Shorter telomeres in dystrophic muscle consistent with extensive regeneration in young children. Neuromuscul Disord 2000, 10:113–120
21. Grounds MD: Age-associated changes in the response of skeletal muscle cells to exercise and regeneration. Ann NY Acad Sci 1998, 854:78–91
22. Wagers AJ, Conboy IM: Cellular and molecular signatures of muscle regeneration: current concepts and controversies in adult myogenesis. Cell 2005, 122:659–667
23. Conboy IM, Conboy MJ, Smythe GM, Rando TA: Notch-mediated restoration of regenerative potential to aged muscle. Science 2003, 302:1575–1577
24. Conboy IM, Conboy MJ, Wagers AJ, Girma ER, Weissman IL, Rando TA: Rejuvenation of aged progenitor cells by exposure to a young systemic environment. Nature 2005, 433:760–764
25. Rabinovsky ED, Gelir E, Gelir S, Lui H, Kattash M, DeMayo FJ, Shenaq SM, Schwartz RJ: Targeted expression of IGF-1 transgene to skeletal muscle accelerates muscle and motor neuron regeneration. FASEB J 2003, 17:53–55
26. Miller KJ, Thaloor D, Matteson S, Pavlath GK: Hepatocyte growth factor affects satellite cell activation and differentiation in regenerating skeletal muscle. Am J Physiol 2000, 278:C174–C181
27. Sheehan SM, Allen RE: Skeletal muscle satellite cell proliferation in response to members of the fibroblast growth factor family and hepatocyte growth factor. J Cell Physiol 1999, 181:499–506
28. Borisov AB, Dedkov EI, Carlson BM: Differentiation of activated satellite cells in denervated muscle following single fusions in situ and in cell culture. Histochem Cell Biol 2005, 124:13–23
29. Chen YW, Nagaraju K, Bakay M, McIntyre O, Rawat R, Shi R, Hoffman EP: Early onset of inflammation and later involvement of TGFβ in Duchenne muscular dystrophy. Neurology 2005, 65:826–834
30. McCroskery S, Thomas M, Platt L, Hennebry A, Nishimura T, McLeay L, Sharma M, Kambadur R: Improved muscle healing through enhanced regeneration and reduced fibrosis in myostatin-null mice. J Cell Sci 2005, 118:3531–3541